DOI: 10.1038/NGEO764

Supplementary Methods

Estuarine Circulation

We estimate the magnitude of the estuarine circulation in the fjord by assuming a simple two-layer system with an outflowing fresh plume and an inflowing saltier layer (Supplementary Figure 1a). Using relations for the conservation of mass and salt[28], the fjord's flushing time (T_f) due to an estuarine circulation is:

$$T_f = \frac{(h_{out} + h_{in})WL}{S_{in}R}(S_{in} - S_{out}),$$

where W is the width of the fjord (8 km), L the length (100 km), R the rate of melt water input, h the layer thickness, S the salinity, and subscripts '*in*/*out*' refer to the inflowing deep, salty layer and the outflowing fresh layer, respectively. If we assume the estuarine circulation is confined to the upper 300m (the layer over which we observed the most pronounced changes), data from the two surveys yield the following estimates: h_{out} ~ 10-20 m, h_{in} ~ 280m, S_{in} ~ 33-33.3, S_{out} ~ 28-29.5.

To estimate meltwater input, R, we first consider Helheim Glacier, the dominant source of meltwater for Sermilik Fjord. Measurements of exposed stake heights on Helheim Glacier (GSH and LAS, unpublished data) yield surface melt rates of ~4 m/yr at 100 m asl and ~2 m/yr at 700 asl. We use a simple linear scaling to apply these estimates to the glacierized area surrounding the upper portion of Sermilik Fjord using a digital elevation model[3] to obtain a liquid water runoff of ~5 Gt/yr. An unknown amount of liquid water is generated by submarine melting at the tidewater terminus of Helheim Glacier and by icebergs in the fjord which, for the purposes of this calculation, we assume is equal to the terrestrial runoff. This yields a net value for R (~10 Gt/yr) which is

probably an underestimate because we neglected 1) snow-melt runoff from the non-glacierized land-surface and 2) meltwater from other portions of the ice sheet bordering the fjord as well as local glaciers. To account for this and, in general, to minimize the flushing time estimate, we more than double our estimated fresh water input and use R~ 25 Gt/yr = 25 km^3/yr.

Using these values, the estimated flushing time of the upper 300 m is > 2 yr, with a mean inflow velocity of 0.1 cm/s and an outflow velocity of 2 cm/s. It would take more than 5 years to flush the entire fjord (assuming a mean depth of 700 m). We emphasize that the purpose of this simple calculation is to maximize the magnitude of the estuarine circulation (and minimize the flushing time); even taking the maximum range of input values yields a flushing time that is an order of magnitude slower than that implied from our field observations. This suggests that, while still contributing to the net circulation within the fjord, the meltwater driven estuarine circulation is not the dominant mechanism for water mass renewal inside the fjord.

Along-shore Winds

12 hourly wind velocity (at 10 m) data are obtained from NASA's Quick Scatterometer (QuikSCAT; http://podaac.jpl.nasa.gov). Winds in the coastal region outside of Sermilik Fjord are derived by averaging across a region bounded by 36-39º W and 64.5-66º N (see Figure 3c). This region is large enough to ensure that data coverage is always available and minimizes the effect of data gaps that commonly occur in the proximity of the coast. We note that the winds over the shelf have relatively large spatial coherence and that our results are not overly sensitive to the exact 'region' used for averaging. Positive along-shore winds are oriented at 54º (see Figure 3c). The wind-stress

DOI: 10.1038/NGEO764

is obtained using the Large and Pond formulation[29] (Figure 4a and Supplementary Figure 2a). Wind events are defined as along-shore wind events whose magnitude exceeds 0.1 N m^{-2} and whose duration is longer than 1 day.

Intermediary Circulation

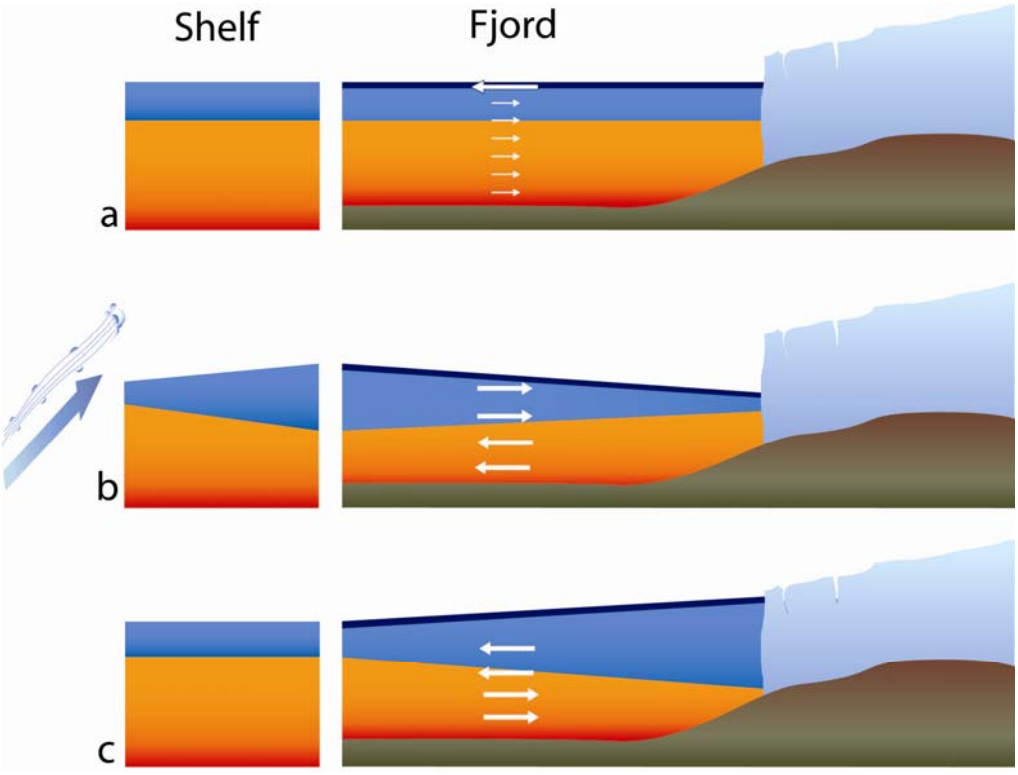

Supplemental Figure 1 Circulation in Sermilik Fjord a) Classic estuarine circulation in the absence of wind-forcing: a fast outflowing glacial meltwater plume and a weaker compensating inflow at depth. Wind-driven circulation: b) Northeasterly winds 'pile-up' water and depress the halocline at the mouth driving an inflow in the upper layer and outflow at depth. c) After the wind ceases and the shelf region returns to pre-event conditions and the fjord relaxes through the reverse circulation.

DOI: 10.1038/NGEO764

Analysis of the 8-month mooring record

The third mooring, carrying a single CTD recorder was deployed in early September 2008 and recovered in mid-August 2009 (see Methods Summary). Its initial location coincided with that of the shallow summer mooring but, after having been hit and displaced by ice several times, the mooring settled at 65 m at the end of December, 40 m deeper than its original depth. Spatially, the mooring was displaced less than 100 m from its original location. To remove any bias due to displacement, we restrict this analysis to data from December 28, 2008 to August 20, 2009 when the mooring remained at one location (and depth). Post-recovery calibrations did not show any sensor drift. The mooring recorded temperature (T), salinity (S) and pressure (P) every half hour throughout its deployment. These data were filtered with a 40 hour Hanning window to remove tidal and other high frequency noise (Supplementary Figure 2 b-d). To quantify the fjord's response to along-shore wind events, which have time-scales on the order of several days, we removed long term variations (such as seasonal) from the records by subtracting a 30-day low-pass filtered time series (also using a 30-day Hanning window). The resulting time series of anomalies are shown in Supplementary Figure 2e. The along shore wind stress outside of the fjord for the same period is shown in Supplementary Figure 2a. An anomaly time series for the wind is obtained in the same way as for the ocean variables, Supplementary Figure 2e.

Visual inspection of the curves in Supplementary Figure 2 shows that positive wind stress anomalies are associated with positive pressure (equivalent to positive sea-surface height), negative salinity, and negative temperature anomalies. This is the expected response for a northeasterly wind event described in the text and Supplementary

DOI: 10.1038/NGEO764

Figure 1 b and c. A simple regression of the anomaly time series for the fjord's properties on the wind stress anomaly time series reveals that all three are significantly correlated at the 99% level using 64 degrees of freedom (193 day long record with a 3-day decorrelation time scale), Supplementary Table 1. The correlation is largest for the pressure record which is representative of sea-surface height variability and at zero lag. (Mooring blow down is negligible given the length of the mooring, less than 1 m, and, also, it cannot account for negative pressure anomalies.) This is consistent with a rapid barotropic adjustment of the fjord. Maximum correlations with temperature and salinity are found at 1 day lag consistently with the slower baroclinic response.

Supplementary Table 1. Correlations of variables from the long mooring record with the alongshore wind stress.

Variable	R	Lag	Significant
Salinity	-0.33	1 day	$p < 0.01$
Temperature	-0.46	1 day	$p < 0.01$
Pressure	0.53	0	$p < 0.01$

Finally, it is evident from Supplementary Figure 2 that the wind-driven intermediary circulations do not account for all of the variability at this depth. Departures from this correlation are expected to occur and, we argue, are not inconsistent with the conclusions of this study – that the wind-driven intermediary circulation is the dominant but not the only forcing of the fjord's variability. Indeed, the mooring discussed here is shallow enough that one cannot rule out the impact of local air-sea fluxes both during the wintertime period (as sea-ice forms in the fjord) and during the summer (when summer

DOI: 10.1038/NGEO764
nature geoscience

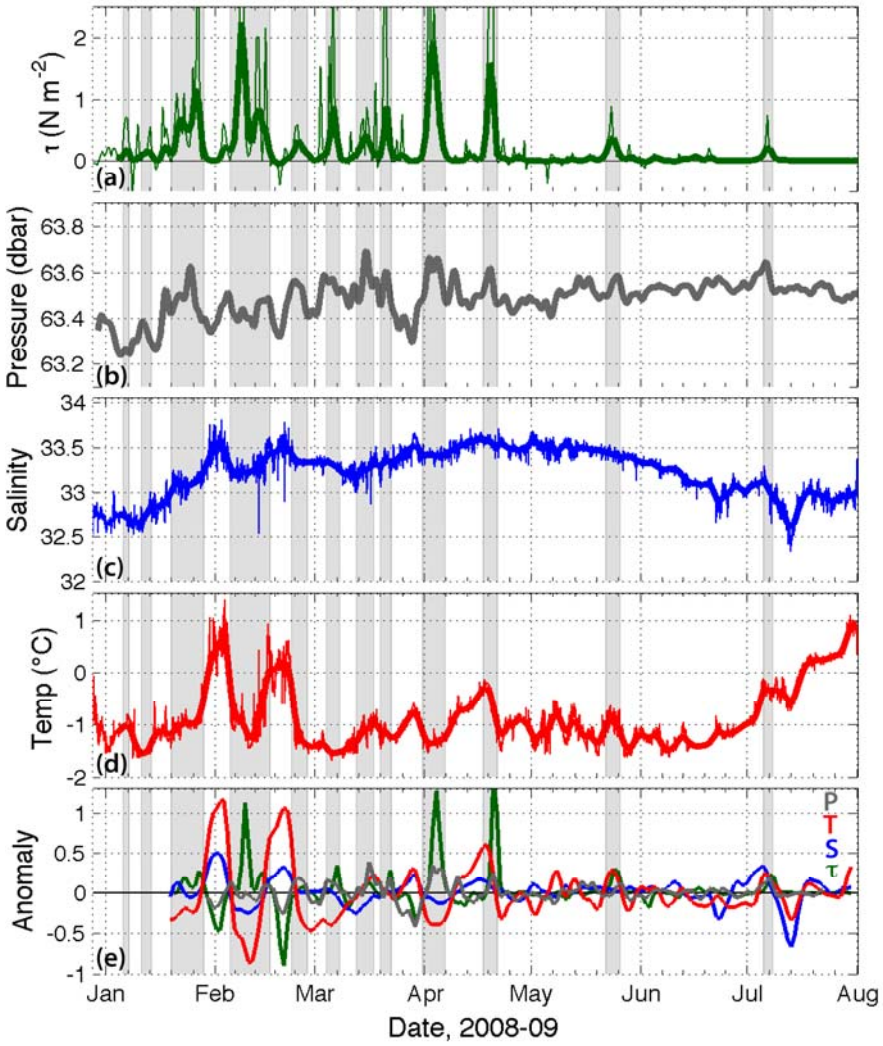

Supplementary Figure 2. (a) Time series of the alongcoast windstress, τ (N m^{-2}), outside Sermilik Fjord measured by the QuikSCAT scatterometer (see Supplementary Methods). The light line is the original data and the heavy line is the 40-hr low-passed time-series. Shading highlights downwelling (τ > 0) wind. (b) The 40-hr low-pass filtered pressure record from the shallow mooring. (c) Same as in *b*, but for salinity. (d) Same as in *b*, but for temperature. (e) Time series of pressure (P), temperature (T), salinity (S), and wind stress (τ) anomalies. The wind stress and pressure anomalies have been shifted one day to correspond with the maximum correlations found with T and S. The τ, S, and P anomalies are scaled by a factor of 2 to help visualization. Units are the same as in panels a) to d).

DOI: 10.1038/NGEO764

heating may be mixed down). The latter may explain the warming observed in late summer when there appear to be few or no wind-events. Second, and as noted in the main text, intermediary circulations will arise from any mechanism that generates a fjord/shelf pressure gradient (e.g. coastally trapped waves or eddies). Indeed on intermediary-circulation-like event occurs in mid-July but it is not associated with a wind-event (Supplementary Figure 2).

References:

28. Knauss, J. A. *Introduction to Physical Oceanography*. 2nd edition, Prentice-Hall, New Jersey, 309 pp (1997)

29. Large, W.G. & Pond, S. Open ocean momentum flux measurements in moderate to strong winds. *J. Phys. Oce*. **11**, 324-336 (1981)